Scientific Frontiers in Research on Extrasolar Planets
ASP Conference Series, Vol. 294, 2003
D. Deming and S. Seager, eds.

Dynamical Instabilities in Extrasolar Planetary Systems

Eric B. Ford

Department of Astrophysical Sciences, Princeton University, Peyton Hall, Ivy Lane, Princeton, NJ 08544

Frederic A. Rasio and Kenneth Yu

Northwestern University, Dept. of Physics & Astronomy, 2145 Sheridan Rd., Evanston, IL 60208-0834

Abstract. Instabilities and strong dynamical interactions between multiple giant planets have been proposed as a possible explanation for the surprising orbital properties of extrasolar planetary systems. In particular, dynamical instabilities seem to provide a natural mechanism for producing the highly eccentric orbits seen in many systems. Previously, we performed numerical integrations for the dynamical evolution of planetary systems containing two giant planets of equal masses initially in nearly circular orbits very close to the dynamical stability limit. We found the ratio of collisions to ejections in these simulations was greater than the ratio of circular orbits to eccentric orbits among the known extrasolar planets. Further, the mean eccentricity of the planets remaining after an ejection was larger than the mean eccentricity of the known extrasolar planets. Recently, we have performed additional integrations, generalizing to consider two planets of unequal masses. Our new simulations reveal that the two-planet scattering model can produce a distribution of eccentricities consistent with the observed eccentricity distribution for plausible mass distributions. Additionally, this model predicts a maximum eccentricity of about 0.8, in agreement with observations. Early results from simulations of three equal-mass planets also reveal a reduced frequency of collisions and a broad range of final eccentricities for the retained inner planet.

1. Background

The known extrasolar planets (Figure 1, left) can be roughly divided into two groups: those with short-period, nearly circular orbits ($a \lesssim 0.07\,\mathrm{AU}$) and those with wider and more eccentric orbits ($a \gtrsim 0.07\,\mathrm{AU}$). Many of the short-period planets, like their prototype 51 Peg, are so close to their parent star that tidal dissipation would have likely circularized their orbits, even if they were originally eccentric (Rasio et al. 1996). Thus, their small observed eccentricities do not provide a good indicator of their dynamical history. However, the large eccentricities of most planets with longer periods require an explanation. A planet that would have formed from a protoplanetary disk in the standard manner is unlikely to have developed such a large eccentricity, since dissipation in the disk tends to circularize orbits. Dynamical instabilities leading to the ejection of one planet while retaining another planet of comparable mass could explain the observed distribution of eccentricities.

In previous papers (Rasio & Ford 1996; Ford, Havlickova, & Rasio 2001), we conducted Monte Carlo integrations of planetary systems containing two equal mass planets initially placed just inside the Hill stability limit (Gladman 1993). We numerically integrated the orbits of such systems until there was a collision, or one planet was ejected from the system, or some maximum integration time was reached. The two most common outcomes were collisions between the two planets, producing a more massive planet in a nearly circular orbit between the two initial orbits, and ejections of one planet from the system while the other planet remains in a tighter orbit with a large eccentricity. The relative frequency of these two outcomes depends on the ratio of the planet radius to the initial semi-major axis. While this model could naturally explain how planets might acquire large eccentricities, upon comparing our results to the observed planets we found two important differences. First, for the relevant radii and semi-major axes, we found that collisions are more frequent in our simulations than nearly circular orbits among the presently known extrasolar planets. Second, of the systems which ended with one planet being ejected from the system, the eccentricity distribution of the remaining planet was concentrated in a narrow range which is greater than the typical eccentricity of the known extrasolar planets (see Figure 1, right). Here we present results for new simulations involving two planets with unequal masses and three planets with equal masses.

2. Two Planets, Unequal Masses

2.1. Numerical Setup

The new simulations use the mixed variable symplectic algorithm (Wisdom & Holman 1991) modified to allow for close encounters between planets as implemented in the publicly available code Mercury (Chambers 1999). The results presented below are based on $\sim 10^4$ numerical integrations.

Throughout the integrations, close encounters between any two bodies were logged, allowing us to present results for any values of the planetary radii using a single set of orbital integrations. We consider a range of radii to allow for the uncertainty in both the physical radius and the effective collision radius allowing for dissipation in the planets. When two planets collided, mass and momentum conservation were used to compute the final orbit of the resulting single planet.

Each run was terminated when one of the following four conditions was encountered: (i) one of the two planets became unbound (which we defined as having a radial distance from the star of $1000\,a_{1,\mathrm{init}}$); (ii) a collision between the two planets occurred assuming $R_i/a_{1,\mathrm{init}} = R_{\mathrm{min}}/a_{1,\mathrm{init}} = 0.1\,R_{\mathrm{Jup}}/5\,\mathrm{AU} = 0.95 \times 10^{-5}$; (iii) a close encounter occurred between a planet and the star (defined by having a planet come within $r_{\mathrm{min}}/a_{1,\mathrm{init}} = 10\,R_{\odot}/1\,\mathrm{AU} = 0.06$ of the star); (iv) the integration time reached $t_{\mathrm{max}} = 5 \cdot 10^6 - 2 \cdot 10^7$ depending on the masses of the planets. These four types will be referred to as "collisions," meaning a collision between the two planets, "ejections," meaning that one

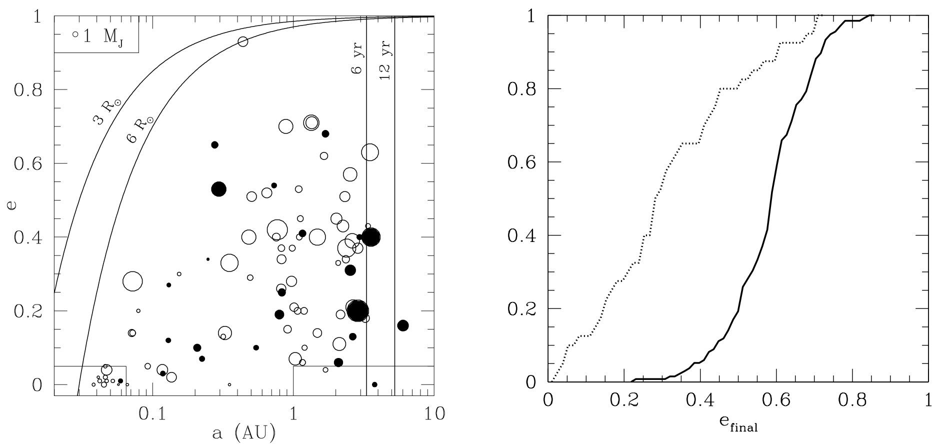

Figure 1. Left: Orbital eccentricity versus semi-major axis of known extrasolar planets. The eccentricity of planets in very short period orbits is limited by tidal damping. Nearly all of the remaining planets have large eccentricities. The area of the circle is proportional to $m \sin i$. Planets represented by shaded circles are part of a multiple planet system. Right: Cumulative distribution of eccentricity. The solid line shows the eccentricity distribution of the remaining planet after the other planet has been ejected from the system in our previous simulations with two planets of equal mass. The dotted line shows the eccentricity distribution of the known extrasolar planets (excluding those with $P < 10$ d). Among systems resulting in an ejection, the final eccentricity is larger than typical for the observed extrasolar planets.

planet was ejected to infinity, "star grazers," meaning that one planet had a close pericenter passage, and "two planets," meaning that two bound planets remained in a (possibly new) dynamically stable configuration.

Our numerical integrations were performed for a system containing two planets, with mass ratios $10^{-4} < m_i/M < 10^{-2}$, where m_i is the mass of one of the planets and M is the mass of the central star. A mass ratio of $m/M \simeq 10^{-3}$ corresponds to $m \simeq 1\,M_{\rm Jup}$ for $M = 1\,M_{\odot}$. The initial semi-major axis of the outer planet ($a_{2,\rm init}$) was drawn from a uniform distribution ranging from $0.9 \cdot a_{1,\rm init}\,(1+\Delta_c)$ to $a_{1,\rm init}\,(1+\Delta_c)$, where $1+\Delta_c$ is the critical ratio above which Hill stability is guaranteed for initially circular coplanar orbits (Gladman 1993). The initial eccentricities were distributed uniformly in the range from 0 to 0.05, and the initial relative inclination in the range from 0° to 2°. All remaining angles (longitudes and phases) were randomly chosen between 0 and 2π. Throughout this paper we quote numerical results in units such that $G = a_{1,\rm init} = M = 1$. In these units, the initial orbital period of the inner planet is $P_1 \simeq 2\pi$.

2.2. Results

Branching Ratios For the range of m_i/M considered (up to 10^{-2}), the frequency of the various outcomes is relatively insensitive to the ratio of the total planet mass to the stellar mass. However the frequencies of the different outcomes are significantly affected by the planetary mass ratio and by the planetary radii. Collisions are most common for large planetary radii and mass ratios near unity, while ejections are most common for small planetary radii and mass ratios far from unity. The frequency of outcomes does not depend on whether the more massive planet is initially in the inner or outer orbit. In Figure 2 (left), we show the frequency of ejection or collision as a function of the planetary radii with solid and dashed lines, respectively. The different lines show the results for the indicated mass ratios. Ejections become more common and collisions less frequent as the planetary mass ratio departs from unity.

Collisions Collisions leave a single, larger planet in orbit around the star. The energy in the center-of-mass frame of the two planets is much smaller than the binding energy of a giant planet. Therefore, we model the collisions as completely inelastic and assume that the two giant planets simply merge together while conserving total momentum and mass. Under this assumption, we have calculated the distributions of orbital parameters for the collision products. The final orbit has a semi-major axis between the two initial semi-major axes, a small eccentricity, and a small inclination. While collisions between planets may affect the masses of extrasolar planets, a single collision between two massive planets does not cause significant orbital migration or eccentricity growth if the planets are initially on low-eccentricity, low-inclination orbits near the Hill stability limit.

Ejections When one planet is ejected from the system, the less massive planet is nearly always ejected if $\frac{m_<}{m_>} \leq 0.8$, where $m_<$ and $m_>$ refer to the masses of the less and more massive planets, respectively. Since the escaping planet typically leaves the system with a very small (positive) energy, energy conservation sets the final semi-major axis of the remaining planet slightly less than

$$\frac{a_f}{a_1} \simeq \frac{a_2\, m_<}{a_1\,(m_1+m_2)+(a_2-a_1)\, m_1}. \tag{1}$$

Thus, the ejection of one of two equal mass planets results in the most significant reduction in the semi-major axis, but is limited to $\frac{a_f}{a_{1,\mathrm{init}}} \geq 0.5$. The remaining planet acquires a significant eccentricity, but its inclination typically remains small. The eccentricity distribution for the remaining planet is not sensitive to the sum of the planet masses, but depends significantly on the mass ratio. In Figure 2 (right) we show the cumulative distributions for the eccentricity after a collision for different mass ratios. While any one mass ratio results in a narrow range of eccentricities, a distribution of mass ratios would result in a broader distribution of final eccentricities. Also note that there is a maximum eccentricity which occurs for equal mass planets. Thus, the two planet scattering model predicts a maximum eccentricity of about 0.8 independent of the distribution of planet masses. While this compares favorably with the presently known planets, future observations will certainly test this prediction.

Stargrazers In a small fraction of our numerical integrations ($\sim 3\%$) one planet underwent a close encounter with the central star. Due to the limitations of the

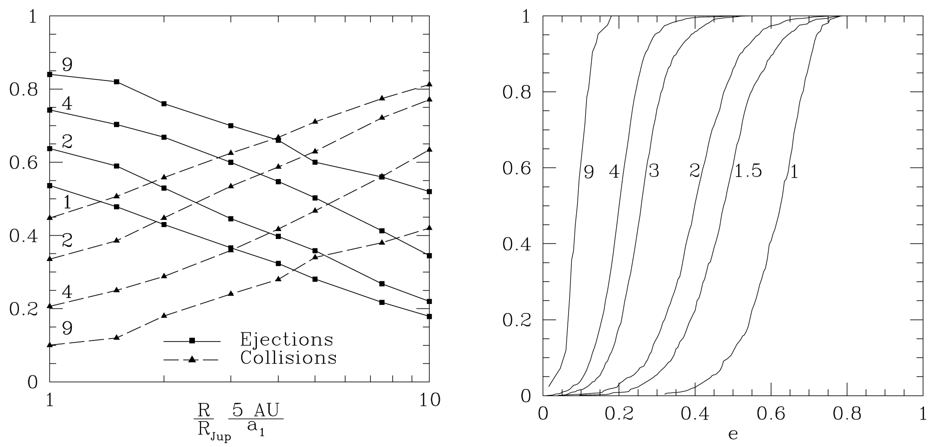

Figure 2. Left: Branching ratio versus planet radius. The frequency of collisions (dashed lines) and ejections (solid lines) depends on the planet's radius relative to the semi-major axis (x-axis) and the planetary mass ratio (numerical labels). The fraction of integrations resulting in one planet being ejected and the other planet remaining in an eccentric orbit is increased when the two planetary masses differ. Right: Cumulative distribution of eccentricity. Each line shows the cumulative distribution of the eccentricity of the remaining planet after the other planet has been ejected from the system in our simulations for a particular mass ratio. The distributions are not sensitive to the total mass of the planets or to which planet is more massive.

numerical integrator used, the accuracy of our integrations for the subsequent evolution of these systems can not be guaranteed. Moreover, these systems could be affected by additional forces (e.g., tidal forces, interaction with the quadrupole moment of the star) that are not included in our simulations and would depend on the initial separation and the radius of the star. Nevertheless, our simulations suggest that for giant planets with initial semi-major axes of a few AU, the extremely close pericenter distances necessary for tidal circularization around a main sequence star (leading to the formation of a 51-Peg-type system) are possible, but rare.

2.3. Discussion

We now consider whether the the two planet scattering model could produce a distribution of eccentricities consistent with that of known extrasolar planets with periods longer than 10 days. In Figure 3 (left) we show the cumulative distribution for the eccentricity of the remaining planet in our simulations. Here we have chosen a simple distribution of planet masses, $P(m) \simeq m^{-1}$ for $1M_{\rm Jup} \leq m \leq 10M_{\rm Jup}$, which is consistent with the mass distribution of the observed extrasolar planets (Tabachnik & Tremaine 2002). The dashed line is just for systems which resulted in an ejection, while the dotted line includes systems which resulted in a collision. Both are reasonably close to the observed distribution shown by the solid line. It should be noted that the mass distribution used for this model has two cutoffs. While the $10 M_{\rm Jup}$ cutoff is supported by observations, the lower cutoff is not constrained by present observations and is unlikely to be physical. Alternative mass distributions differing for $m \leq 1 M_{\rm Jup}$ could alter this result. A detailed comparison to observations would require the careful consideration of observational selection effects, as well as the unknown initial mass distributions. Nevertheless, we find that the two-planet scattering model is able to reproduce the eccentricity distribution of the known extrasolar planets for plausible mass distributions.

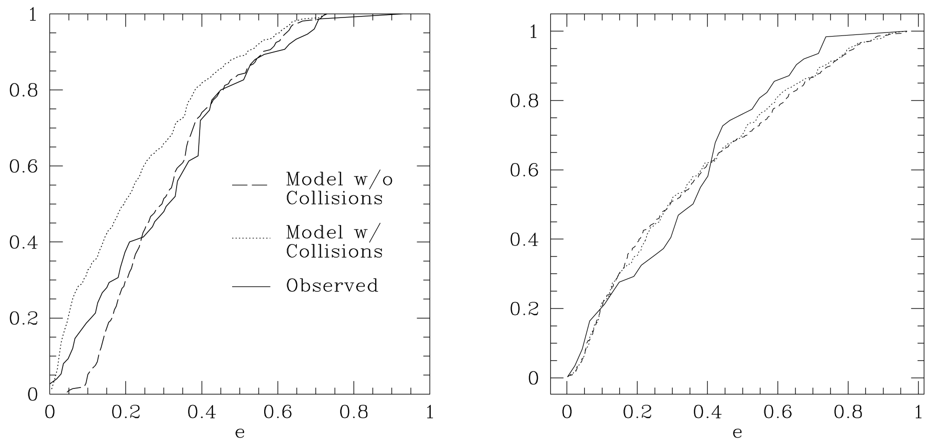

Figure 3. Left: Simulation with mass distribution. Here we compare the observed distribution of eccentricities (excluding planets with $P < 10\,$d, solid line) to the eccentricity distributions produced by our simulations when each planet's mass is drawn independently from $P(m) \sim m^{-1}$ for $1\,M_{\rm Jup} < m < 10\,M_{\rm Jup}$. The dashed line shows the eccentricity of the planet remaining after an ejection, while the dotted line includes systems resulting in a collision. Right: Results from simulations for 3 equal-mass planets. Here we compare the observed distribution of eccentricities (excluding those with $P < 10\,$d, solid line) to the eccentricity distribution of the remaining inner planet after there has been one ejection or collision for one of two sets of simulations with different initial eccentricities. The dashed and dotted lines are for simulations with $e_{\rm init} = 0.$ and $e_{\rm init} = 0.05$, respectively.

3. Three Planets, Equal Masses

We have begun performing simulations of unstable systems containing three equal-mass planets using the conservative Bulirsch-Stoer integrator in Mercury (Chambers 1999). The results presented here are based on $\sim 10^3$ numerical integrations. For three-planet systems, we set the radius of each planet at the beginning of the integration. For determining when collisions occurred, each planet was assigned a radius of $R_i = R_{\rm Jup}$. A planet was removed from the system if its separation from the central star became greater than 1000AU (ejected) or less than $r_{\rm min} = R_\odot$ (collided with star).

For three-planet systems, a single ejection or collision results in a system containing two planets. The remaining two planets may either be dynamically stable or undergo a subsequent ejection or collision to end with a single planet. Each run was terminated when two of the planets were removed by being ejected, colliding with another planet, or colliding with the star, or when the maximum integration time was reached $t_{\rm max} = 2 \times 10^6$ years.

Our numerical integrations were performed for a system containing three planets, each with a mass ratio $m/M \simeq 10^{-3}$. The initial semi-major axes are fixed at 1, 1.39, and 1.92 AU, so that the ratio of orbital periods is $P_3/P_2 = P_2/P_1 = 1.63$. Each planet is initially placed on a nearly circular orbit with an eccentricity of either 0.0 or 0.05 and an inclination of $\pm 1°$. All remaining angles (longitudes and phases) were randomly chosen between 0 and 2π.

The typical time for instability to develop is $\sim 10^6$ years. In the majority of cases, two planets were left in a stable configuration after one planet was ejected or two planets collided. In Figure 3 (right) we show the distributions of the eccentricity of the inner planet after a collision or ejection of one planet. It is in reasonable agreement with the observed distribution for extrasolar planets. Both the eccentricity distribution (Figure 3, right) and the corresponding distribution of the inclination of the inner planet (Figure 4, left) are in qualitative agreement with those presented by Marzari & Weidenschilling (2002, based on slightly different initial conditions). In Figure 4 (right) we show the cumulative distribution for $\Delta\varpi = |(\Omega_2 + \omega_2) - (\Omega_1 + \omega_1)|$, the angle between the periapses of the two planets remaining after one planet has been ejected from the system. We do not find the two remaining planets to have preferentially aligned periapses (cf. Malhotra 2002).

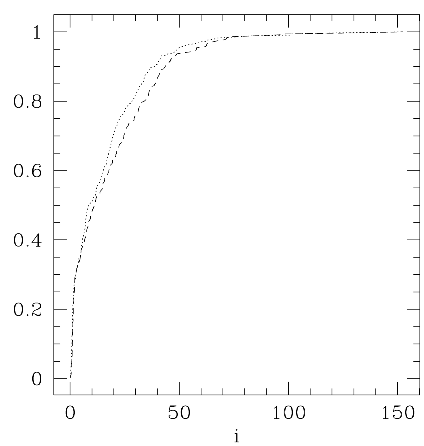

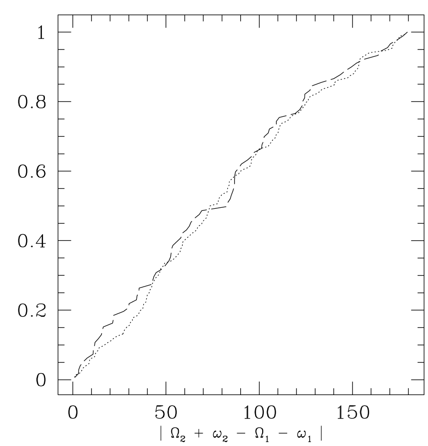

Figure 4. Left: Cumulative distribution of inclination. Each line shows the distribution of the inclination of the remaining inner planet (with respect to the initial orbital plane) after there has been one ejection or collision for one of two sets of simulations with different initial eccentricities. The dashed and dotted lines are for simulations with $e_{\rm init} = 0.$ and $e_{\rm init} = 0.05$, respectively. Right: Cumulative distribution of the periapse misalignment angle between two retained planets.

4. Conclusions

Dynamical interactions between planets of unequal mass reduces the frequency of collisions as compared to scattering between equal-mass planets. In particular, planet-planet scattering can reproduce the observed distribution of eccentric orbits using a plausible distribution of mass ratios. To determine if collisions are sufficiently rare will require a more careful comparison to the observations. Independent of the distribution of planet masses, planet-planet scattering by two planets initially on nearly circular orbits produces a maximum eccentricity of ~ 0.8. While this compares favorably with the presently known extrasolar planets, future detections will test this prediction of the two-planet scattering model. Alternatively, the observed properties of extrasolar planets could also be produced as a result of dynamical instabilities developing in three-planet systems.

Acknowledgments. We are grateful to Eugene Chiang, Renu Malhotra, and Scott Tremaine for valuable discussions. E.B.F. acknowledges the support of the NSF graduate research fellowship program and Princeton University, and thanks the Theoretical Astrophysics group at Northwestern University for hospitality. F.A.R. and K.Y. acknowledge support from NSF grant AST-0206182. Our computations were supported by the National Computational Science Alliance under Grant AST980014N and utilized the SGI/Cray Origin2000 supercomputers at Boston University.

References

Chambers, J. E. 1999, MNRAS, 304, 793

Chambers, J. E., Wetherill, G. W., & Boss, A. P. 1996, Icarus, 119, 261

Ford, E. B., Havlickova, M., & Rasio, F. A. 2001, Icarus, 150, 303

Gladman, B. 1993, Icarus, 106, 247

Lin, D. N. C. & Ida, S. 1997, ApJ, 447, 781

Malhotra, R. 2002, ApJ, L33

Marzari, F. & Weidenschilling, S. J. 2002, Icarus, 156, 570

Rasio, F. A. & Ford, E. B. 1996, Science, 274, 954

Rasio, F. A., Tout, C. A., Lubow, S. H., & Livio, M. 1996, ApJ, 470, 1187

Tabachnik, S. & Tremaine, S. 2002, MNRAS, 335, 151

Weidenschilling, S. J. & Marzari, F. 1996, Nature, 384, 619

Wisdom, J. & Holman, M. 1991, AJ, 102, 1528